crystals

MDPI

Article

Preparation of Memantine-Loaded Chitosan Nanocrystals: In Vitro and Ex Vivo Toxicity Analysis

Mohamed A. Saleh [1,2], Jamal M. M. Mohamed [3], J. Joysa Ruby [4], Selvakumar Kanthiah [5], Yasmene F. Alanazi [6], Kamlah A. Majrashi [7], Sultan M. Alshahrani [8], Mohamed Ahmed Eladl [9], Fatima S. Alaryani [10], Mohamed El-Sherbiny [11,12,*] and Farid Menaa [13,*]

1 Department of Clinical Sciences, College of Medicine, University of Sharjah, Sharjah 27272, United Arab Emirates
2 Department of Pharmacology and Toxicology, Faculty of Pharmacy, Mansoura University, Mansoura 33516, Egypt
3 Vaasudhara College of Pharmacy, Hoskote 562114, India
4 Department of Pharmaceutics, Acharya & BM Reddy College of Pharmacy, Bengaluru 560107, India
5 Department of Pharmaceutical Analysis, Acharya & BM Reddy College of Pharmacy, Bengaluru 560107, India
6 Department of Biochemistry, Faculty of Science, University of Tabuk, Tabuk 71421, Saudi Arabia
7 Department of Biological Sciences, College of Science & Arts, King Abdulaziz University, Rabigh 21911, Saudi Arabia
8 Department of Clinical Pharmacy, College of Pharmacy, King Khalid University, Abha 61441, Saudi Arabia
9 Department of Basic Medical Sciences, College of Medicine, University of Sharjah, Sharjah 27272, United Arab Emirates
10 Department of Biology, College of Science, University of Jeddah, Jeddah 21589, Saudi Arabia
11 Department of Basic Medical Sciences, College of Medicine, AlMaarefa University, Riyadh 11597, Saudi Arabia
12 Department of Anatomy and Embryology, Faculty of Medicine, Mansoura 35511, Egypt
13 Department of Nanomedicine, California Innovations Corporation, San Diego, CA 92037, USA
* Correspondence: msharbini@mcst.edu.sa (M.E.-S.); menaateam@gmail.com (F.M.)

check for updates

Citation: Saleh, M.A.; Mohamed, J.M.M.; Ruby, J.J.; Kanthiah, S.; Alanazi, Y.F.; Majrashi, K.A.; Alshahrani, S.M.; Eladl, M.A.; Alaryani, F.S.; El-Sherbiny, M.; et al. Preparation of Memantine-Loaded Chitosan Nanocrystals: In Vitro and Ex Vivo Toxicity Analysis. *Crystals* **2023**, *13*, 21. https://doi.org/10.3390/cryst13010021

Academic Editor: Pavel Lukáč

Received: 11 October 2022
Revised: 18 December 2022
Accepted: 20 December 2022
Published: 23 December 2022

Copyright: © 2022 by the authors. Licensee MDPI, Basel, Switzerland. This article is an open access article distributed under the terms and conditions of the Creative Commons Attribution (CC BY) license (https://creativecommons.org/licenses/by/4.0/).

Abstract: Alzheimer's disease (AD) is a progressive neurodegenerative disorder with unmet medical need, and is the leading cause of age-related dementia affecting millions of people worldwide. This work aims at developing small, high-drug loading capacity (DL) and -entrapment efficiency (EE) memantine hydrochloride (MEM)/chitosan nanocrystals (CS-NCs) to treat moderate to severe dementia associated with AD. MEM-loaded chitosan nanocrystals (MEM/CS-NCs, further abbreviated as MEM-NCs) were prepared by the ionic gelation method. Different formulations were prepared by varying the concentrations of CS and sodium tripolyphosphate (STPP). The prepared MEM-NCs formulations (n = 8) were evaluated for their particle size (PS), polydispersibility index (PDI), zeta potential (ZP), DL, EE and characterized by scanning electron microscopy (SEM) and transmission electron microscopy (TEM). Furthermore, in vitro (i.e., release behavior, cytotoxicity) and ex vivo studies (i.e., histopathology) studies were carried out. The results show that the DL was over 92% and the EE was higher than 73%, while the particles were relatively small with nanometric PS (152.63 ± 12.95 to 310.23 ± 10.49 nm), uniform with acceptable PDI (0.336 ± 0.05 to 0.534 ± 0.02), and stable with positive ZP (23.8 ± 0.4 mV to 54.0 ± 0.5 mV). The optimal formulation (MEM-NC3) was selected mainly based on the PS (152.63 ± 12.95 nm), DL (98.44 ± 3.31%), and EE (78.7 ± 3.11%). Interestingly, it does not elicit any cytotoxic and tissue damage when examining at goat nasal mucosa. The selected formulation was subjected to surface morphological studies such as transmission electron microscopy (TEM), which revealed that the NCs were spherical in shape and small (100 nm). Interestingly, the selected formulation was able to sustain the drug release for up to 24 h with an initial burst release (86.51 %). We conclude that the prepared MEM-NCs represent a promising drug formulation for further in vivo studies (in animal models and in a clinical setting) to prevent and treat AD.

Keywords: memantine HCl/chitosan nanocrystals; ionic gelation method; Alzheimer's disease; neurodegenerative disorder; nanomedicine; innovation

1. Introduction

AD is the fourth largest cause of death for people over the age of 65 years; it is defined as a neurodegenerative disorder characterized by irreversible and progressive memory loss followed by complete dementia [1,2]. The cognitive decline is characterized by impaired daily activity performance, speech, behavior, and visual-spatial perception. Cognitive impairment in AD is caused by death of cholinergic neurons in basal forebrain area. Thereby, a deficit of acetylcholine (ACh) contributes substantially to the etiology of AD [1,2]. At the same time, the level of dementia correlates with the extent of neuronal death caused by an excess of glutamate which is considered as the most prevalent excitatory neurotransmitter in the brain to date [2].

Memantine hydrochloride (MEM HCl, simply abbreviated as MEM) is the hydrochloride salt form of memantine, voltage-dependent non-competitive and N-methyl-D-aspartate (NMDA) receptor antagonist [3]. MEM binds and inhibits the cationic channels of glutaminergic NMDARs (NMDA receptors) channel located in the central nervous system (CNS); this channel is classified as an open channel blocker' as it can enter and block the current only when the channel is opened [3]. It is also both a nicotinic receptor antagonist and a 5-hydroxytryptamine type 3 (5HT3) receptor antagonist. MEM is used to treat moderate to severe dementia associated with AD [3].

All the N-methyl-D-aspartate (NMDA) receptor antagonists available nowadays are taken orally, but about 57–82% of the unchanged drug gets eliminated in the urine [4]. Moreover, the gastrointestinal side effects of these NMDA inhibitors included nausea, anorexia, muscle spasms, and diarrhea. When MEM is administered intravenously (IV), the onset of effects is very rapid. The parenteral route has also its own limitations; it is not a patient-friendly route because of the possibility of adverse reactions and fear of the needles. However, other delivery strategies, including intranasal administration (nasal route), may outperform oral dosages [5], and could be considered as an alternative to treat AD. By this administration route, MEM could prevent the prolonged influx of calcium ions, neuronal cytotoxicity and thus enhances the cognitive function [6]. Therefore, to treat AD, it remains imperative to create long-term, non-gastrointestinal delivery strategies for these NMDA inhibitors. Brain delivery by nose, via the olfactory pathway, by bypassing the blood–brain barrier (BBB), appears the best route for fast onset of action, increased bioavailability, and decreased side effects when treating AD with MEM.

Chitosan (CS) is rich in amino and hydroxyl (positively charged) groups, which facilitate the formation of nanoparticles (NPs) by chemical and physical cross-linking (hydrogen bonding in aqueous solution). The positively charged groups of CS can be ionically cross-linked by electrostatic interactions (non-covalent) with negatively charged counter ions like those found in the non-toxic and multivalent tripolyphosphate (TPP) anion [7–9]. In the present study, ionic gelation method was used to implement the preparation of MEM-CS NCs.

The distribution of medications through the BBB is one of the biggest issues in the treatment of AD. The inclusion of anti-AD drugs in polymeric nanoparticles (NPs) is a viable remedy for these issues. While many polymeric NPs are biocompatible and nontoxic, many of them cannot be used for CNS targeting because they are not biodegradable [10]. CS-based NPs stand out among polymeric drug nanocarriers which are both stable and biodegradable delivery systems for CNS. Indeed, CS has garnered interest as a non-toxic, safe, stable, and promising natural polymer for use in drug delivery systems. In recent years, a great deal of research has been done to design drug delivery systems that use CS to treat different neurological illnesses [11]. Additionally, because of their mucoadhesive properties and inherent bioactivity, CS NPs can both facilitate drug absorption into the brain through the olfactory pathway and can be used as nanocarriers of anti-AD drugs. With a focus on improving BBB penetration of AD drugs and minimizing their peripheral adverse effect, CS-based NPs might be employed to overcome certain obstacles in the treatment of AD [12].

Drugs are protected by polymeric NPs by entrapment inside the core, encapsulation, adsorption on the particle surface or conjugation. Polymeric NPs have several advantages over other NPs, including a low quantity requirement of drug, higher stability, ease of synthesis, extended and sustained drug release profile, biodegradability, biocompatibility, nontoxicity, minimal drug alteration, prolonged blood circulation period, and the ability to deliver drugs to specific sites or the brain [13]. Polymeric NPs use endocytosis and transcytosis mechanisms to transport molecules with payload across the BBB. Some polymeric NPs, such as CS, polybutylcyanoacrylate (PBCA), dendrimers, and poly(d,l-lactide-co-glycolide) (PLGA),are helpful in drug delivery and therapy of brain illnesses [14]. Chitin polymer, which is widely accessible and has several medicinal uses, is used to create CS NPs. With longer plasma circulation times, these modified NPs were able to pass the BBB via transferrin receptor-mediated endocytosis. CS NPs can deliver caspase-3 inhibitor using this method, preventing ischemia-induced apoptosis in neuronal cells [15]. Recently, Rocha-Meneses et al. demonstrated that functionalized CS NPs loaded with large peptide moieties and brain-targeted anti-transferrin monoclonal antibody were able to rapidly penetrate BBB and elicit neuroprotection [16].

Among the several synthetic methods, NP synthesis using ion exchange is a flexible and effective method that offers a new route to designing complicated structures and metastable NPs, which are not accessible by standard syntheses [17]. Due to their adaptability and capacity to modify fine structures, NP syntheses by ion exchange reactions are anticipated to be able to produce novel devices with necessary characteristics.

In recent years, nasal route is considered as convenient, safe, non-invasive, and reliable route for brain targeting. Drug will reach the brain by nasal cavity via olfactory and trigeminal nerves present in nasal cavity. Though polymeric nanocrystals (PNCs) have been used widely for oral, parenteral, ocular, and transdermal delivery, recently, brain targeting through PNCs via nasal route has also increased [18]. A particle range between 1 and 100 nm in size with a consistent atomic structure is referred to as an NC. There are amorphous NPs and those made of two or more NCs.

The novelty of the present investigation is related to the development of small, uniform, and stable PNCs for a drug used to treat AD (i.e., Memantine) while improving targeted and sustained/controlled delivery of the drug to the brain. PNCs are designed to overcome issues encountered with conventional dosage forms (e.g., standard formulations such multidose treatment, substandard patient compliance, and high cost). Indeed, the hydrophilic nature of MEM cannot pass the BBB; a PS of less than 200 nm is also a key requirement for crossing this barrier. Therefore, MEM-CS NCs was selected as the carrier in this study to assess in vitro and ex vivo analyses before any in vivo studies.

2. Materials and Methods

2.1. Reagents

Memantine HCl (MEM) was purchased from Hetero Drugs, Hyderabad, India. Chitosan (CS) 400 kD MW and sodium tripolyphosphate (STPP) 85% deacetylated were bought from Sigma Aldrich, Mumbai, India. The other chemicals and regents used in this study were of analytical grade.

2.2. Preparation of Memantin-Loaded Chitosan Nanocrystals (MEM-NCs)

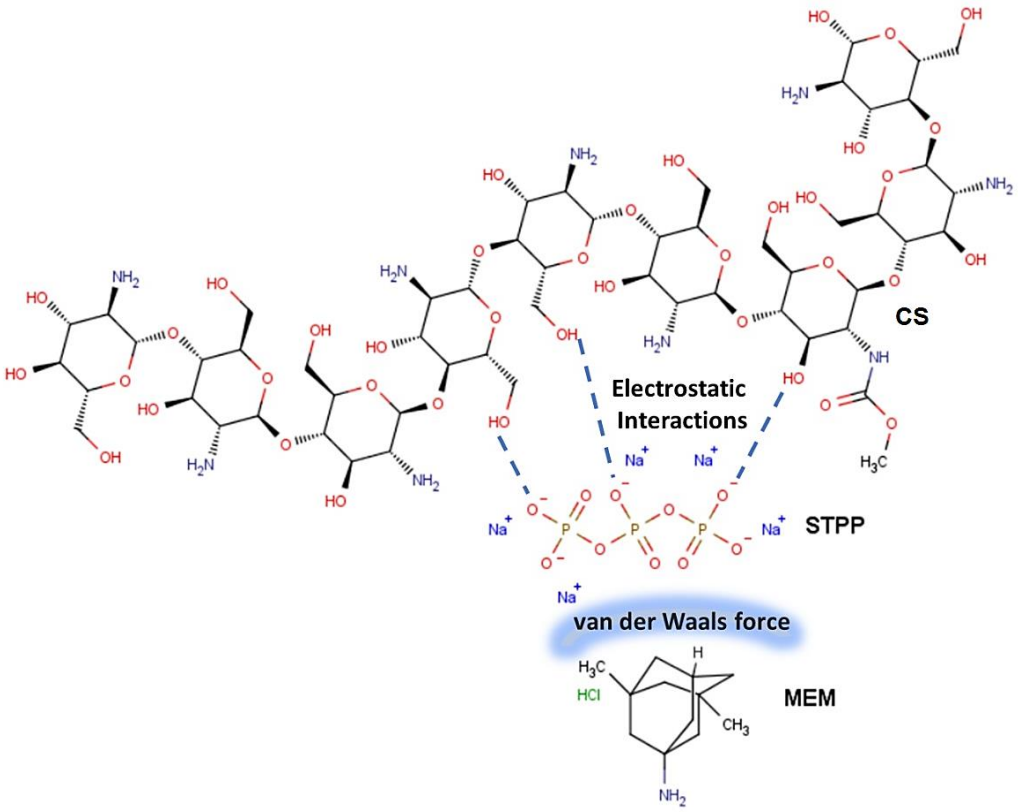
High-quality (Supplementary file) MEM-NCs were prepared by ionic gelation method. The CS- MEM solution was prepared by using different concentration of polymer-drug ratio (Table 1). The CS concentration ranged from 2 to 9 mg. STPP was dissolved in water to get clear solution. The prepared STPP solution was added dropwise to CS- MEM solution using 1 mL micro syringe and was stirred at 1000 rpm using a magnetic stirrer (REMI 2). The resulting solution was then filtered by using a membrane filter (0.45 µm; Millipore) to remove the residual from STPP. The obtained NCs were concentrated by ultracentrifugation at 12,000 rpm at 4 °C for 20 min [19].

Table 1. Various formulation concentration and condition of MEM-NCs.

Formulation Code	MEM Concentration (mg)	CS: MEM Concentration Ratio	Time (h)
MEM-NC1	10	2:1	4
MEM-NC2	10	3:1	4
MEM-NC3	10	4:1	4
MEM-NC4	10	5:1	4
MEM-NC5	10	6:1	4
MEM-NC6	10	7:1	2
MEM-NC7	10	8:1	6
MEM-NC8	10	9:1	6

MEM: memantine HCl; CS: chitosan; NC: nanocrystal.

Electrostatic interactions were present between the CS and STPP. Here, the oxygen atoms of the STPP show electrostatic interaction with the OH group of the CS (Scheme 1). Further, the STPP interacted with the MEM by van der Waals forces. The major alkyl groups of MEM show van der Waals forces with the electronegative oxygen atoms of the STPP [20].



Scheme 1. Schematic diagram of the chemical reactions between MEM, STPP, and CS.

2.3. Particle Size (PS), Polydispersibility Index (PDI) and Zeta Potential (ZP)

A light scattering PS analyzer was used to measure the PS and PS distribution (PSD) of the prepared MEM-NCs with appropriate dilutions according to the method described by Mohamed et al. (2022). All samples were measured at least three times. The measurements of ZP and PDI are frequently employed to forecast the stability of a nanosystem. Nano ZS, a product of Malvern Instruments, Malvern, UK, was used to calculate ZP of the prepared MEM-NCs [21].

2.4. Drug Entrapment Efficiency (EE) and Drug Loading (DL)

Freeze dried MEM-NCs were dissolved in acetonitrile and filtered (0.45 µm membrane filter) and the solution were estimated using UV-Vis spectrophotometer at 291 nm (UV-Vis method performance parameters such as accuracy, precision, repeatability, and linearity are mentioned in the supplementary file). EE and DL of MEM were quantified using following Equations [22]:

$$(\%)EE = \frac{quantity\ of\ MEM\ in\ NCs}{quantity\ of\ MEM\ in\ the\ preparation} \times 100 \quad (1)$$

$$(\%)\mathrm{DL} = \frac{quantity\ of\ MEM\ in\ NCs}{quantity\ of\ NCs\ ontained} \times 100 \quad (2)$$

2.5. Morphology

2.5.1. Scanning Electron Microscopy

High magnification was used for SEM, which produces high-resolution pictures and accurately quantifies very minute features and objects. SEM micrographs of pure MEM and MEM-NCs were obtained by spreading a small quantity of powdered sample over a double-sided carbon tape on a metal study, then the sample was gold coated (ion sputter) to form a thin layer over it and mounted into a SEM microscope (Carl Zeiss Microscopy Ltd., Cambridge, UK). A working distance of ~5 mm with acceleration of 10.0 kV were applied, and images at various levels of magnification were captured [23].

2.5.2. Transmission Electron Microscopy (TEM)

The morphology of selected MEM-NCs was investigated after they were diluted with Milli Q water (1:1000), placed on a copper grid, and air dried [16]. The sample was further investigated using a TEM (FEI Technai TF-30, Hillsboro, OR) at 200 kV after being negatively stained with a 1% solution of phosphotungstic acid.

2.6. Powder X-ray Diffraction (PXRD) Studies

The XRD analysis was used to investigate the impact on the crystallinity of MEM and MEM-NCs by using a diffractometer (Siemens D5000, Munich, Germany). The samples were put into a sample holder that used Cu Kα radiation as its source. The diffractometer was then operated at 40 kV and 30 mA current [24]. The samples were scanned at a speed of 3° per minute with a step size of 0.02° over an angle range of 0° to 80°.

2.7. In Vitro Release Studies

The in vitro drug release study was performed using the dialysis bag method. Nanocrystals equivalent to 5 mg of the drug was placed in a cellulose dialysis bag, (MWCO 12,000 g/mole) and to this a little amount of dissolution media (PBS) was added, which was then sealed at both ends. It was then placed in a beaker containing 1× PBS at pH 6.4. Aliquots of 5 mL were withdrawn at each interval of time and were replaced with fresh dissolution media. The samples were measured by UV spectrophotometer at 291 nm [25].

2.8. In Vitro Cell Cytotoxicity Using RPMI 2650 Cell Lines

To measure the growth modulation of cells, tetrazolium salt 3-(4, 5 dimethyl thiazole-2-yl)-2, 5-diphenyl tetrazolium bromide (MTT) assay was carried out using RPMI 2650 cell line. The RPMI 2650 cell line was treated with different concentration of MEM-NCs and pure MEM solution ranging 62.5 mg/mL to 1000 mg/mL for 72 h. After 72 h, the cell lines were microscopically examined for morphological changes [26].

2.9. Ex Vivo Histopathological Studies

Ex vivo histopathological studies were carried out on goat nasal mucosa (conchae nasals). Freshly isolated goat nasal mucosa was stored in 1× PBS (pH 6.4) and cut into

four defined pieces of uniform thickness and diameter. Each section was named as negative control, positive control, pure MEM solution and MEM-NCs [27]. PBS (pH 6.4) was used as negative control, isopropyl alcohol (IPA) as positive control, drug solution (2 mg/mL) and MEM NCs dispersion (2 mg/mL), respectively. The nasal mucosa, treated for 72 h, was stored, and examined on an optical microscope to detect any toxicity by examining the potential damages to the tissues.

2.10. Statistical Analysis

The results of each experiment were performed in triplicate and are shown as mean standard deviation (mean ± SD, $n = 3$). The data were analyzed using one-way analysis of variance (ANOVA), with a significance level of $p < 0.05$.

3. Results and Discussion

3.1. PS, PDI, ZP, DL, and EE of MEM-NCs: MEM-NC3 as the Optimal Formulation

In the solution, MEM-NCs were found to have a bi-modal size distribution (complex including at least two molecules) with a hydrodynamic PS in the range of 152.63 ± 12.95 to 310.23 ± 10.49 nm and a PDI of 0.336 ± 0.05 to 0.534 ± 0.02 (Table 2). ZP of MEM-NCs ranged between 23.8 ± 0.4 mV and 54.0 ± 0.5 mV (Table 2).

Table 2. Basic physical characteristics of MEM–NCs. * Each value signifies mean ± SD, $n = 3$; the significant variances compared to control (pure MEM) are denoted by ** $p < 0.05$, as estimated by the ANOVA test. Otherwise, $p > 0.05$.

Formulation Code	PS (nm) *	PDI *	ZP (mV) *	DL * (%)	EE * (%)
MEM-NC1	204.90 ± 14.09	0.359 ± 0.03	28.6 ± 1.40	96.22 ± 5.32	76.6 ± 3.55 **
MEM-NC2	158.96 ± 8.63 **	0.534 ± 0.02	23.8 ± 0.40	94.63 ± 3.64	74.6 ± 4.59
MEM-NC3	152.63 ± 12.95 **	0.437 ± 0.14	36.1 ± 0.60	98.44 ± 3.31 **	78.7 ± 3.11 **
MEM-NC4	310.23 ± 10.49	0.437 ± 0.06	54.0 ± 0.50 **	95.66 ± 4.64	74.5 ± 5.43
MEM-NC5	211.76 ± 6.10	0.336 ± 0.05	45.3 ± 1.20	92.57 ± 5.32	75.4 ± 2.69
MEM-NC6	278.46 ± 16.77	0.370 ± 0.17	50.1 ± 2.80	94.85 ± 5.78	74.9 ± 5.67
MEM-NC7	212.90 ± 4.78	0.342 ± 0.05	47.5 ± 1.60	95.55 ± 6.76	73.8 ± 4.80
MEM-NC8	290.70 ± 7.60	0.474 ± 0.18	52.1 ± 1.50 **	94.87 ± 5.11	73.8 ± 5.77

MEM: memantine HCl; NC: nanocrystal; PS: particle size; PDI: polydispersibility index; ZP: zeta potential; DL: drug loading content/capacity; EE: drug loading/entrapment efficiency.

MEM-NC-3 displayed the smallest PS (Table 2). This formulation displayed a hydrodynamic diameter of 152.63 ± 12.95 nm with a PDI of 0.437 ± 0.14 (Figure 1a). ZP is a crucial metric for understanding the makeup of the particle surface and determining the stability of the complex over time [28]. The ZP of MEM-NC-3 was estimated to be 36.1 ± 0.6 (Figure 1b), which demonstrates that the surface charge was somewhat reduced. Due to the MEM being entirely encased by the CS shell, MEM-NC-3 was able to exert an enough repulsive force to prevent settling or aggregation/agglomeration during long-term storage, as indicated by the reported low PDI value (<0.7), which indicates the homogeneity in PSD [29,30].

DL (%) and EE (%) of MEM-NCs ranged between 92.57 ± 5.32 % and 98.44 ± 3.31%, and between 73.8 ± 5.77 and 78.7 ± 3.11%, respectively (Table 2). The maximum absorption of MEM-NCs, measured between 200 and 400 nm, with a peak at 291 nm, was responsible for nearly 90% of the overall output maintained ($p > 0.05$). This value was within the reference (label quantity) range of 90 to 105% of MEM. MEM-NC3 displayed the highest DL (98.44 ± 3.31%) and EE (78.7 ± 3.11%), and so was selected as optimal formulation for these parameters (in addition to its smallest size). The drug:polymer ratio of MEM-NC3

was 1:4 (MEM:CS). A lipophilic drug may improve EE by integrating a positively charged carrier like CS, as claimed by Senthilvel et al. (2022) [31].

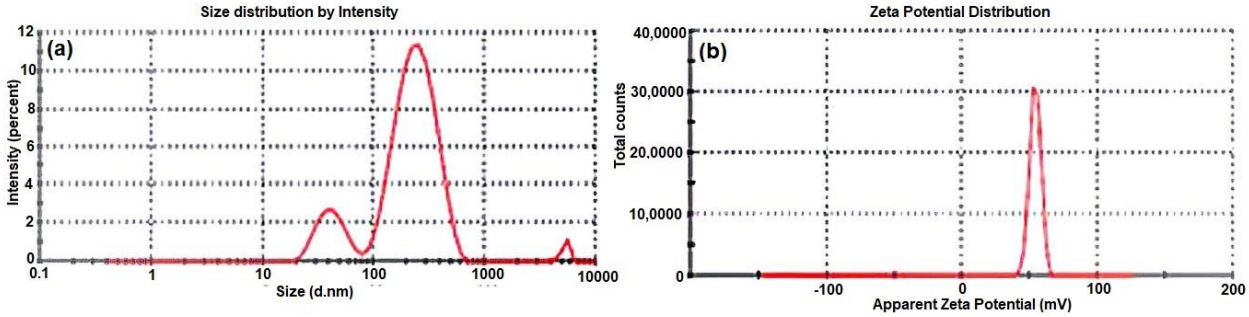


Figure 1. (**a**) PS and (**b**) ZP of the optimized formulation (MEM-NC3).

3.2. Surface Morphology of MEM-NC3 by SEM Depicts Smooth Spherical NPs

The surface morphologies of free MEM and MEM-NC3 (selected as optimal formulation) are depicted in Figure 2. The free MEM appears smooth and crystalline with an average particle size of 15 µm (Figure 2a). MEM-NC3 was spherical with a crystalline surface and a PS in the nanometric range was confirmed (Figure 2b). The formation of an encircling crystal network by a thin polymer layer during hydration enables the system to transform from globular to spherical and achieve thermodynamic stability by lowering total free energy [32]. The stability of the spherical structure was demonstrated even when several mechanical stressors, such as sonication and ultracentrifugation, were used.

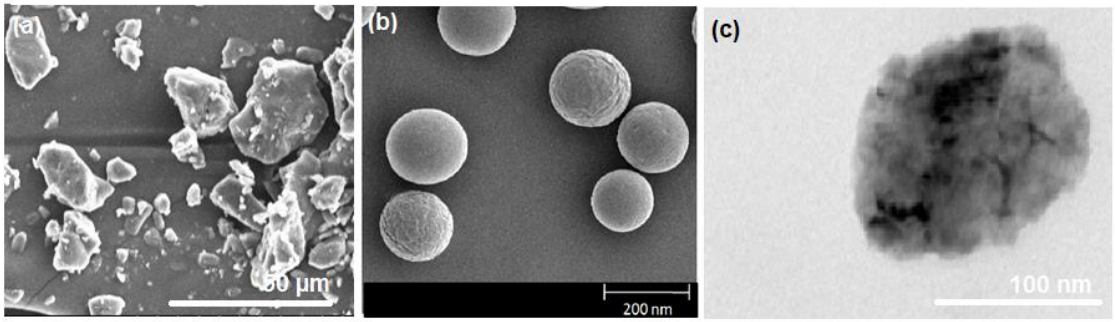


Figure 2. SEM image of (**a**) free MEM, (**b**) MEM-NC3, and (**c**) TEM image of MEM-NC3.

The morphology of freshly prepared MEM-NC3 indicates that nanocrystals were roughly spherical in shape with size ranges of 100–129 nm (Figure 2c). MEM-NC3 regularly exhibited a smooth spherical form with a dense CS matrix that is homogenous (PDI of 0.437), however the size is smaller than the hydrodynamic measurement as determined by dynamic light scattering [33].

3.3. PXRD of MEM-NC3 Revealed Its Crystalline Nature

A typical method for identifying a novel crystallographic phase in the solid/crystal state is PXRD. The diffraction patterns of pure MEM and MEM-NC3 crystals are shown in Figure 3. Characteristic diffraction peak of 2θ values were visible in the PXRD pattern for pure MEM at 11.01, 14.98, 19.04, 26.11, and 30.83°. On the other hand, MEM-NC3 displayed several distinctive interference peaks with 2θ values at 11.89, 13.65, 12.90, 17.06, 18.41, and 20.44°. The formation of a new crystalline peak was confirmed as CS characteristic peaks and the lack of the MEM peaks was observed (characteristic peak of CS was slightly altered with 2θ values at 10.78 and 19.25°). This study confirmed that the prepared MEM-NC3 was crystals [28,34,35].

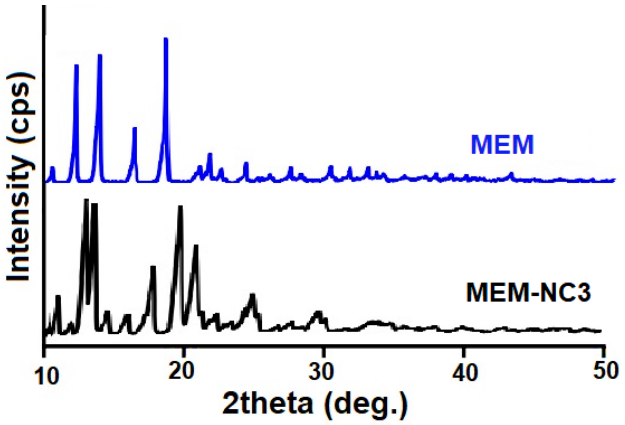


Figure 3. PXRD pattern of MEM and MEM-NC3 (aka MEM/CS-NC3).

3.4. In Vitro Release Study Showed Sustained and Controlled Release of MEM-NC3

The in vitro release behavior of pure MEM and MEM-NCs is shown in Figure 4. An initial drug release of 21.44 ± 1.21% was observed, which may be accounted for the MEM adsorbed to the surface. After 12 h, 78.51 ± 2.21 % of MEM was released, followed by slow release up to 24 h with 87.28 ± 2.01 %. The increased release in aqueous media from 21.44 ± 1.21% to 87.28 ± 2.01 % is due to the swelling property of the polymer. Further, there was no significant release found among the tested MEM-NCs and up to 24 h. The optimized formulation MEM-NC3 displayed a higher but insignificant ($p < 0.05$) release rate compared to that of other formulation. The MEM-NCs showed biphasic pattern of release with an initial burst release followed by a sustained release markedly enhanced ($p < 0.05$) as compared to the pure MEM (control), which is a BCS-I drug (high solubility, high permeability). CS has been referred to be more efficient at enhancing drug uptake when formulated in the nanocrystal form, as compared to solution [28,34,35]. Thereby, MEM-NCs (aka MEM/CS-NCs) could release the MEM in a regulated way over the course of 24 h, meantime strongly suggesting that CS may have affected MEM release from NCs. It could be able to offer a continuous/uninterrupted drug release over a longer length of time because of MEM enhanced solubility [36].

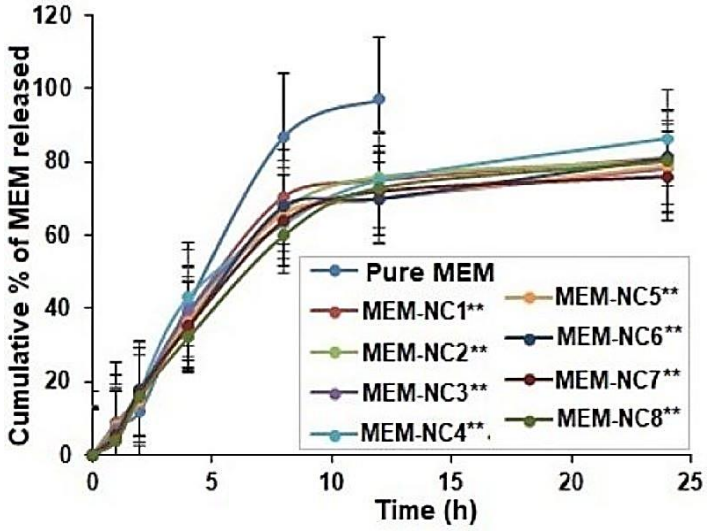


Figure 4. Cumulative percentage of MEM released from various MEM-NCs (mean ± SD, n = 3); the significant variances associated with control (pure MEM) are denoted by ** $p < 0.05$, as estimated by the ANOVA test.

3.5. Cytotoxicity Studies Showed that Lower Doses MEM-NC3 are Safer Compared to Pure MEM

The cytotoxicity of pure MEM and MEM-NPs have been investigated for their antiproliferative activity in human nasal cell line RPMI 2650 based on MTT assay [37]. The RPMI 2650 cell line was treated with different concentrations (62.5 µg/mL to 1000 mg/mL) of MEM-NC3 (test) or pure MEM (control) solution for 72 h. MEM-NC3 showed markedly lower cytotoxicity ($p < 0.05$) as compared to the pure MEM. RPMI 2650 cell lines exposed to MEM and MEM-NP after 72 h of treatment exhibited increased cytotoxicity in a dose-dependent manner (Figure 5). As per this study, a dose of MEM-NC3 up to 250 mg/mL^{-1} is recommended. Nevertheless, such a study in additional cell lines (like brain cells) and kinetic studies at doses lower than 500 mg/mL^{-1} are to be performed.

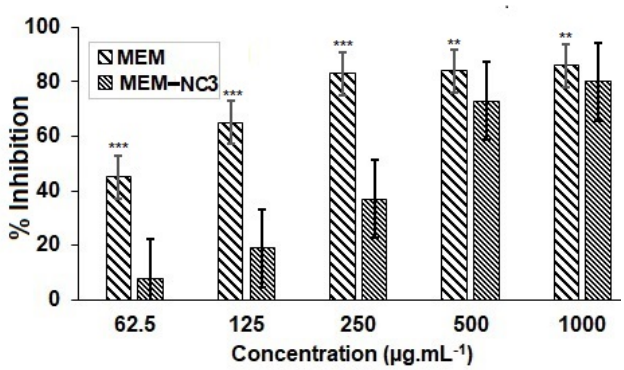


Figure 5. Percentage inhibition of RPMI 2650 cells on pure MEM and MEM-NC3 at various concentrations (mean ± SD, $n = 3$). The significant variances associated with control (pure MEM) are denoted by *** $p< 0.005$ and ** $p< 0.05$ as estimated by the ANOVA test.

Their morphological changes were microscopically examined (Figure 6), which confirmed cytotoxic effects of MEM and MEM-NC3 when the dose is at least as high as 500 mg/mL. Microscopic images of RPMI 2650 cells exposed to MEM and MEM-NCs after 72 h of treatment exhibited significant cytotoxicity in a dose-dependent manner, which are in line with our previous MTT findings.

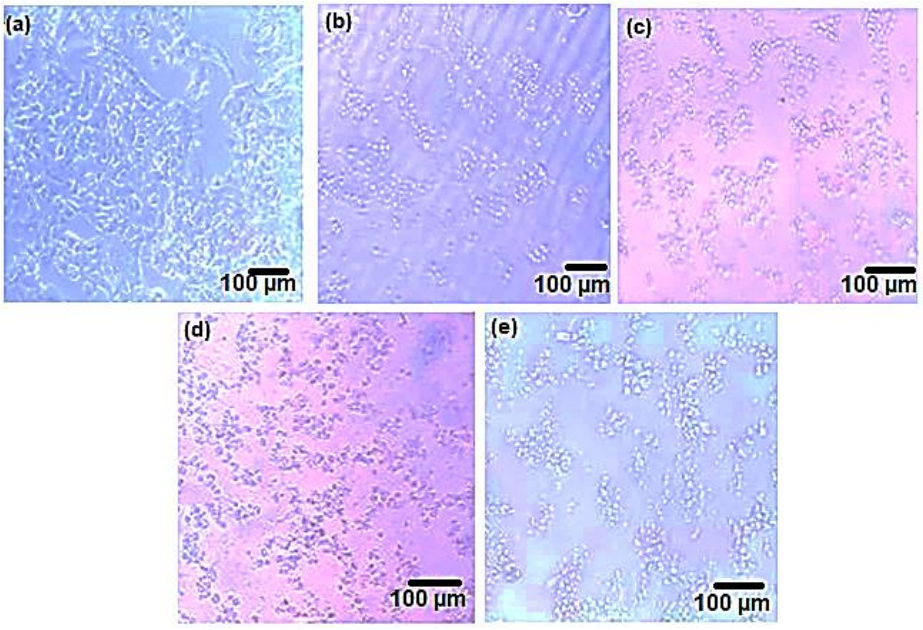


Figure 6. In vitro cytotoxicity microscopic observations of RPMI 2650 cells after 72 h of treatment (**a**) control, (**b**) MEM 1000 µg/mL, (**c**) MEM 500 µg/mL, (**d**) MEM-NC3 1000 µg/mL, and (**e**) MEM-NC3 500 µg/mL.

3.6. Ex Vivo Histopathological Studies Confirm the Safe Use of MEM-NC3 by Nasal Route

The nasal ciliotoxicity study revealed the microscopic structure of the goat nasal mucosa after its treatment for 72 h with PBS (pH 6.4) as a negative control (Figure 7a), IPA, as a positive control (Figure 7b), pure MEM solution, as an internal control (Figure 7c), and MEM-NC3 dispersion, as the selected test (optimal) formulation (Figure 7d). As expected, PBS at physiological pH induced normal tissue architecture of the goat nasal mucosa while IPA induced complete detachment of cilia, loss of epithelial cells, and shrinkage of the mucosal layer of epithelial cells [38]. The drug solution also induced detachment of a few cilia from the epithelial tissue, which indicates toxicity effect when compared with PBS-treated nasal mucosa slides [39,40]. Interestingly, there was no cell necrosis or cilia detachment from the MEM-NC3 dispersion-treated nasal mucosa (Figure 7d).

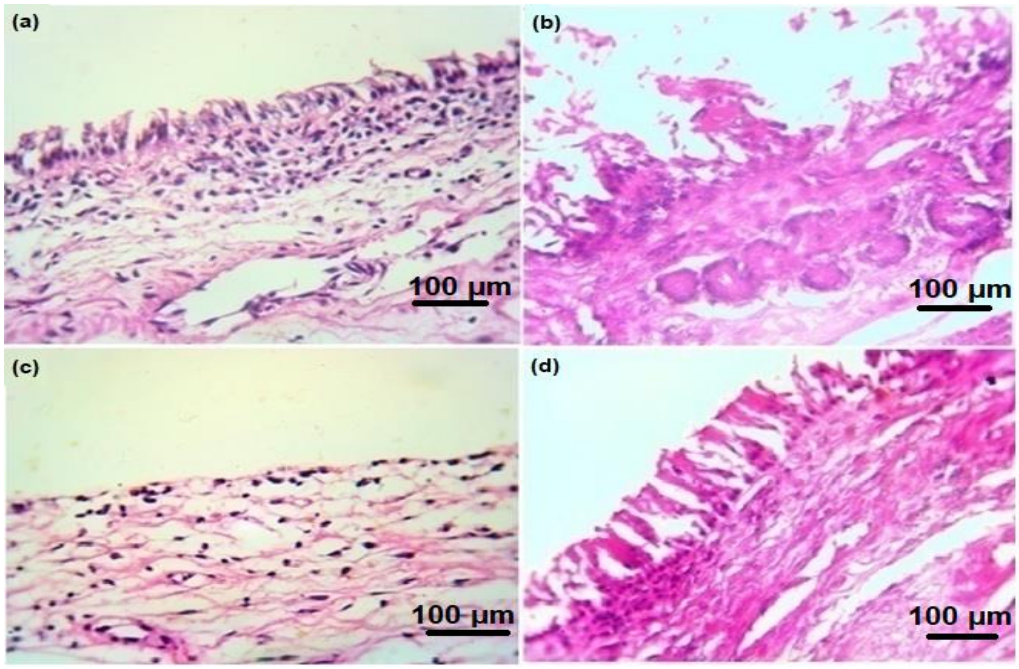


Figure 7. Histopathological images of goat nasal mucosa (**a**) PBS (pH 6.4) negative control, (**b**) IPA positive control, (**c**) pure MEM (2 mg/mL), and (**d**) MEM-NC3 (2 mg/mL).

Overall, these data suggest that a dose higher than 500 µg/mL^{-1} (0.5 mg/mL) and at least up to 2000 µg/mL (2 mg/mL) of MEM-NCs can be administrated via the nasal route in animals without significative adverse effects, and could be more beneficial than the use of free/pure MEM. As nasal administration is a direct route to the brain [41,42], the present study should undergo additional investigations to prove the efficacy (efficiency and safety) of MEM HCl/CS NCs and/or natural neuroprotective plant extracts/phytochemicals entrapped to CS NCs in vivo, using animal models such as *Globodera pallida* [1,2,43] but also to investigate the effects in brain tissues of vertebrates. This pioneered work is a step forward toward a possible solution to prevent and treat more efficiently neurodegenerative diseases.

4. Conclusions

MEM/CS-NCs were successfully prepared by the ionic gelation method (using STTP as a cross-linker). The optimized MEM-NC3 formulation was characterized both in vitro and ex vivo. MEM/CS-NC3 (abbreviated as MEM-NC3) displayed smooth, spherical uniform, stable NCs. Interestingly, MEM could be released in a controlled/sustained manner in vitro. Furthermore, MEM-NC3 represents a potential new strategy for safe MEM nasal delivery since MEM-NC3 were significantly less cytotoxic than pure MEM at the tested concentrations both in treated human nasal RPMI 2650 cells and goat nasal mucosa tissue. These findings represent a first few steps forward in the development

of a novel nasal delivery system for the treatment of Alzheimer's disease, among other neurodegenerative diseases.

Author Contributions: Conceptualization, investigation, writing—original version: M.A.S., J.M.M.M., J.J.R., S.K., M.E.-S. and F.M.; Methodology, Software: M.A.S., J.M.M.M., J.J.R., S.K., Y.F.A., K.A.M., S.M.A., F.S.A., M.E.-S. and F.M.; funding acquisition, resources, visualization: M.A.E., Y.F.A., K.A.M., S.M.A., F.S.A., M.E.-S. and F.M. Data curation, formal analysis, statistics, writing—review, editing, and validation: M.A.S., J.M.M.M., Y.F.A., K.A.M., S.M.A., M.A.E., F.S.A. and F.M.; Supervision: J.M.M.M., M.E.-S. and F.M.; Submission: J.M.M.M. and F.M. All authors have read and agreed to the published version of the manuscript.

Funding: The work was supported by Research supporting program (MA-006), AlMaarefa University, Riyadh, Saudi Arabia.

Institutional Review Board Statement: Not applicable.

Informed Consent Statement: Not applicable.

Data Availability Statement: Data sharing not applicable.

Acknowledgments: The authors are grateful to the Department of Clinical Sciences, College of Medicine, University of Sharjah, Sharjah 27272, and United Arab Emirates for providing necessary facilities to develop this research work.

Conflicts of Interest: The authors declare no conflict of interest.

References

1. Althobaiti, N.A.; Menaa, F.; Albalawi, A.E.; Dalzell, J.J.; Warnock, N.D.; Mccammick, E.M.; Alsolais, A.; Alkhaibari, A.M.; Green, B.D. Assessment and Validation of *Globodera pallida* as a Novel In Vivo Model for Studying Alzheimer's Disease. *Cells* **2021**, *10*, 2481. [CrossRef] [PubMed]
2. Althobaiti, N.A.; Menaa, F.; Dalzell, J.J.; Albalawi, A.E.; Ismail, H.; Alghuthaymi, M.A.; Aldawsari, R.D.; Iqbal, H.; McAlinney, C.; Green, B.D. Ethnomedicinal Plants with Protective Effects against Beta-Amyloid Peptide (Aβ)1-42 Indicate Therapeutic Potential in a New In Vivo Model of Alzheimer's Disease. *Antioxidants* **2022**, *11*, 1865. [CrossRef] [PubMed]
3. Kuns, B.; Rosani, A.; Varghese, D. Memantine. 2022. Available online: https://www.ncbi.nlm.nih.gov/books/NBK500025/ (accessed on March 2021).
4. Maekawa, Y.; Hasegawa, S.; Ishizuka, T.; Shiosakai, K.; Ishizuka, H. Pharmacokinetics and Bioequivalence of Memantine Tablet and a New Dry Syrup Formulation in Healthy Japanese Males: Two Single-Dose Crossover Studies. *Adv. Ther.* **2019**, *36*, 2930–2940. [CrossRef]
5. Liu, J.; Chang, L.; Song, Y.; Li, H.; Wu, Y. The Role of NMDA Receptors in Alzheimer's Disease. *Front. Neurosci.* **2019**, *13*, 43. [CrossRef] [PubMed]
6. Olivares, D.; Deshpande, V.K.; Shi, Y.; Lahiri, D.K.; Greig, N.H.; Rogers, J.T.; Huang, X. N-methyl D-aspartate (NMDA) receptor antagonists and memantine treatment for Alzheimer's disease, vascular dementia, and Parkinson's disease. *Curr. Alzheimer Res.* **2012**, *9*, 746–758. [CrossRef] [PubMed]
7. Mohammed, M.A.; Syeda, J.T.M.; Wasan, K.M.; Wasan, E.K. An Overview of Chitosan Nanoparticles and Its Application in Non-Parenteral Drug Delivery. *Pharmaceutics* **2017**, *9*, 53. [CrossRef] [PubMed]
8. Yanat, M.; Schroën, K. Preparation methods and applications of chitosan nanoparticles; with an outlook toward reinforcement of biodegradable packaging. *React. Funct Polym.* **2021**, *161*, 1381–5148. [CrossRef]
9. Hoang, N.H.; Le Thanh, T.; Sangpueak, R.; Treekoon, J.; Saengchan, C.; Thepbandit, W.; Papathoti, N.K.; Kamkaew, A.; Buensanteai, N. Chitosan Nanoparticles-Based Ionic Gelation Method: A Promising Candidate for Plant Disease Management. *Polymers* **2022**, *14*, 662. [CrossRef] [PubMed]
10. Li, X.; Tsibouklis, J.; Weng, T.; Zhang, B.; Yin, G.; Feng, G.; Cui, Y.; Savina, I.N.; Mikhalovska, L.; Sandeman, S.R.; et al. Nano carriers for drug transport across the blood–brain barrier. *J. Drug Target.* **2017**, *25*, 17–28. [CrossRef]
11. Shayganfard, M. A Review on Chitosan in Drug Delivery for Treatment of Neurological and Psychiatric Disorders. *Curr. Pharm. Biotechnol.* **2022**, *23*, 538–551. [CrossRef]
12. Manek, E.; Darvas, F.; Petroianu, G.A. Use of Biodegradable, Chitosan-Based Nanoparticles in the Treatment of Alzheimer's Disease. *Molecules* **2020**, *25*, 4866. [CrossRef] [PubMed]
13. Kamaly, N.; Yameen, B.; Wu, J.; Farokhzad, O.C. Degradable Controlled-Release Polymers and Polymeric Nanoparticles: Mechanisms of Controlling Drug Release. *Chem. Rev.* **2016**, *116*, 2602–2663. [CrossRef] [PubMed]
14. La Barbera, L.; Mauri, E.; D'Amelio, M.; Gori, M. Functionalization strategies of polymeric nanoparticles for drug delivery in Alzheimer's disease: Current trends and future perspectives. *Front. Neurosci.* **2022**, *16*, 939855. [CrossRef] [PubMed]

15. Sardoiwala, M.N.; Kaundal, B.; Choudhury, S.R. Chapter 37—Development of Engineered Nanoparticles Expediting Diagnostic and Therapeutic Applications Across Blood–Brain Barrier. In *Micro and Nano Technologies, Handbook of Nanomaterials for Industrial Applications*; Hussain, C.M., Ed.; Elsevier: Amsterdam, The Netherlands, 2018; pp. 696–709.
16. Rocha-Meneses, L.; Hari, A.; Inayat, A.; Shanableh, A.; Abdallah, M.; Ghenai, C.; Shanmugam, S.; Kikas, T. Application of nanomaterials in anaerobic digestion processes: A new strategy towards sustainable methane production. *Biochem. Eng. J.* **2022**, *188*, 108694. [CrossRef]
17. Cho, G.; Park, Y.; Hong, Y.K.; Ha, D. Ion exchange: An advanced synthetic method for complex nanoparticles. *Nano Converg.* **2019**, *6*, 17. [CrossRef] [PubMed]
18. Li, Y.; Wang, C.; Zong, S.; Qi, J.; Dong, X.; Zhao, W.; Wu, W.; Fu, Q.; Lu, Y.; Chen, Z. The Trigeminal Pathway Dominates the Nose-to-Brain Transportation of Intact Polymeric Nanoparticles: Evidence from Aggregation-Caused Quenching Probes. *J. Biomed. Nanotechnol.* **2019**, *15*, 686–702. [CrossRef]
19. Abdelgawad, A.M.; Hudson, S.M. Chitosan nanoparticles: Polyphosphates cross-linking and protein delivery properties. *Int. J. Biol. Macromol.* **2019**, *136*, 133–142. [CrossRef]
20. Zhou, H.X.; Pang, X. Electrostatic Interactions in Protein Structure, Folding, Binding, and Condensation. *Chem. Rev.* **2018**, *118*, 1691–1741. [CrossRef]
21. Mohamed, J.M.M.; Mahajan, N.; El-Sherbiny, M.; Khan, S.; Al-Serwi, R.H.; Attia, M.A.; Altriny, Q.A.; Arbab, A.H. Ameliorated Stomach Specific Floating Microspheres for Emerging Health Pathologies Using Polymeric Konjac Glucomannan-Based Domperidone. *BioMed Res. Int.* **2022**, *2022*, 1–12. [CrossRef]
22. Mohamed, J.M.; Alqahtani, A.; Ahmad, F.; Krishnaraju, V.; Kalpana, K. Stoichiometrically governed curcumin solid dispersion and its cytotoxic evaluation on colorectal adenocarcinoma cells. *Drug Des. Deliv. Ther.* **2020**, *14*, 4639–4658. [CrossRef]
23. Mohamed, J.M.; Alqahtani, A.; Ahmad, F.; Krishnaraju, V.; Kalpana, K. Pectin co-functionalized dual layered solid lipid nanoparticle made by soluble curcumin for the targeted potential treatment of colorectal cancer. *Carbohydr. Polym.* **2020**, *252*, 117180. [CrossRef] [PubMed]
24. Riaz, S.; Fatima Rana, N.; Hussain, I.; Tanweer, T.; Nawaz, A.; Menaa, F.; Janjua, H.A.; Alam, T.; Batool, A.; Naeem, A.; et al. Effect of Flavonoid-Coated Gold Nanoparticles on Bacterial Colonization in Mice Organs. *Nanomaterials* **2020**, *10*, 1769. [CrossRef] [PubMed]
25. Moideen, J.M.M.; Alqahtani, A.; Venkatesan, K.; Ahmad, F.; Krisharaju, K.; Gayasuddin, M.; Shaik, R.A. Application of the Box-Behnken design for the production of soluble curcumin: Skimmed milk powder inclusion complex for improving the treatment of colorectal cancer. *Food Sci. Nutr.* **2020**, *8*, 6643–6659. [CrossRef] [PubMed]
26. Khan, Z.U.; Razzaq, A.; Khan, A.; Rehman, N.U.; Khan, H.; Khan, T.; Khan, A.U.; Althobaiti, N.A.; Menaa, F.; Iqbal, H.; et al. Physicochemical Characterizations and Pharmacokinetic Evaluation of Pentazocine Solid Lipid Nanoparticles against Inflammatory Pain Model. *Pharmaceutics* **2022**, *14*, 409. [CrossRef]
27. Blocker, S.J.; Cook, J.; Mowery, Y.M.; Everitt, J.I.; Qi, Y.; Hornburg, K.J.; Cofer, G.P.; Zapata, F.; Bassil, A.M.; Badea, C.T.; et al. Johnson GA. Ex Vivo MR Histology and Cytometric Feature Mapping Connect Three-dimensional in vivo MR Images to Two-dimensional Histopathologic Images of Murine Sarcomas. Radiol. Imaging. *Cancer* **2021**, *3*, e200103.
28. Mohamed, J.M.M.; Alqahtani, A.; Menaa, F.; Kayarohanam, S.; Fatease, A.A.; Alqahtani, T.; Alamri, A.; El-Sherbiny, M.; Ramkanth, S.; Janakiraman, A.K. In Vitro Physical Characterizations and Docking Studies on Carvedilol Nanocrystals. *Crystals* **2022**, *12*, 988. [CrossRef]
29. Khan, B.A.; Khalid, H.; Khan, M.K.; Hosny, K.M.; Khan, S.; Rizg, W.Y.; Safhi, A.Y.; Halwani, A.A.; Almehmady, A.M.; Menaa, F. Biodegradable Polymers-Based Smart Nanocrystals for Loxoprofen Delivery with Enhanced Solubility: Design, Fabrication and Physical Characterizations. *Polymers* **2022**, *4*, 3464. [CrossRef]
30. Akhtar, N.; Akhtar, N.; Menaa, F.; Alharbi, W.; Alaryani, F.S.S.; Alqahtani, A.M.; Ahmad, F. Fabrication of Ethosomes Containing Tocopherol Acetate to Enhance Transdermal Permeation: In Vitro and Ex Vivo Characterizations. *Gels* **2022**, *8*, 335. [CrossRef]
31. Senthilvel, C.K.; Karuppaiyan, K.; Pothumani, A.; Vedharethinam, A.; Jose, A.W.; Mohamed, J.M.M.; Sherbiny, M.E.; Ebrahim, H.A.; Shafey, M.E.; Dejene, M. Development of Atorvastatin Calcium Biloaded Capsules for Oral Administration of Hypercholesterolemia. *Evid. Based. Complement. Alternat. Med.* **2022**, *2022*, 4995508. [CrossRef]
32. Elhassan, G.O.; Mohamed, J.M.M. Development and in vitro evaluation of valsartan-loaded resealed erythrocytes. *Int. J. Appl. Pharm.* **2022**, *14*, 201–205. [CrossRef]
33. Kamaraj, N.; Rajaguru, P.Y.; Issac, P.K.; Sundaresan, S. Fabrication, characterization, in vitro drug release and glucose uptake activity of 14-deoxy, 11, 12-didehydroandrographolide loaded polycaprolactone nanoparticles. *Asian J. Pharm. Sci.* **2017**, *12*, 353–362. [CrossRef] [PubMed]
34. Zafar, N.; Uzair, B.; Niazi, M.B.K.; Menaa, F.; Samin, G.; Khan, B.A.; Iqbal, H.; Menaa, B. Green Synthesis of Ciprofloxacin-Loaded Cerium Oxide/Chitosan Nanocarrier and its Activity Against MRSA-Induced Mastitis. *J. Pharm. Sci.* **2021**, *110*, 3471–3483. [CrossRef]
35. Iqbal, H.; Khan, B.A.; Khan, Z.U.; Razzaq, A.; Khan, N.U.; Menaa, B.; Menaa, F. Fabrication, physical characterizations and in vitro antibacterial activity of cefadroxil-loaded chitosan/poly(vinyl alcohol) nanofibers against *Staphylococcus aureus* clinical isolates. *Int. J. Biol. Macromol.* **2020**, *144*, 921–931. [CrossRef] [PubMed]
36. Papich, M.G.; Martinez, M.N. Applying Biopharmaceutical Classification System (BCS) Criteria to Predict Oral Absorption of Drugs in Dogs: Challenges and Pitfalls. *AAPS J.* **2015**, *17*, 948–964. [CrossRef]

37. Horváth, T.; Bartos, C.; Bocsik, A.; Kiss, L.; Veszelka, S.; Deli, M.A.; Újhelyi, G.; Szabó-Révész, P.; Ambrus, R. Cytotoxicity of Different Excipients on RPMI 2650 Human Nasal Epithelial Cells. *Molecules* **2016**, *21*, 658. [CrossRef] [PubMed]
38. Selvarajah, J.; Saim, A.M.; Idrus, R.B.H.; Lokanathan, Y. Current and Alternative Therapies for Nasal Mucosa Injury: A Review. *Int. J. Mol. Sci.* **2020**, *21*, 480. [CrossRef] [PubMed]
39. Mohamed, J.M.M.; Khan, B.A.; Rajendran, V.; El-Sherbiny, M.; Othman, G.; Hussamuldin, A.B.A.; Al-Serwi, R.H. Polymeric Ethosomal Gel Loaded with Nimodipine: Optimisation, Pharmacokinetic and Histopathological Analysis. *Saud Pharm J.* **2022**, *30*, 1603–1611. [CrossRef]
40. Khan, M.K.; Khan, B.A.; Uzair, B.; Iram Niaz, S.; Khan, H.; Hosny, K.M.; Menaa, F. Development of Chitosan-Based Nanoemulsion Gel Containing Microbial Secondary Metabolite with Effective Antifungal Activity: In vitro and in vivo Characterizations. *Int. J. Nanomed.* **2021**, *16*, 8203–8219. [CrossRef]
41. Trenkel, M.; Scherließ, R. Nasal Powder Formulations: In-Vitro Characterisation of the Impact of Powders on Nasal Residence Time and Sensory Effects. *Pharmaceutics* **2021**, *13*, 385. [CrossRef]
42. Shah, B.M.; Misra, M.; Shishoo, C.J.; Padh, H. Nose to brain microemulsion-based drug delivery system of rivastigmine: Formulation and ex-vivo characterization. *Drug Deliv.* **2015**, *22*, 918–930. [CrossRef]
43. Althobaiti, N.A.; Menaa, F.; Dalzell, J.J.; Green, B.D. *Globodera pallida*, a non-transgenic invertebrate as a new model for investigating Alzheimer's diease (and other proteinopathies)? *Neural Regen. Res.* **2023**, *18*, 113–114. [CrossRef] [PubMed]

Disclaimer/Publisher's Note: The statements, opinions and data contained in all publications are solely those of the individual author(s) and contributor(s) and not of MDPI and/or the editor(s). MDPI and/or the editor(s) disclaim responsibility for any injury to people or property resulting from any ideas, methods, instructions or products referred to in the content.